

## A PREDICTION OF THE CORONAL STRUCTURE OF THE 21 AUGUST 2017 GREAT AMERICAN SOLAR ECLIPSE

DIBYENDU NANDY,<sup>1,2</sup> PRANTIKA BHOWMIK,<sup>1</sup> ANTHONY R. YEATES,<sup>3</sup> SUMAN PANDA,<sup>1,2</sup> RAJASHIK TARAFDER,<sup>1</sup> AND SOUMYARANJAN DASH<sup>1</sup>

<sup>1</sup>*Center of Excellence in Space Sciences India, Indian Institute of Science Education and Research Kolkata, Mohanpur 741246, West Bengal, India*

<sup>2</sup>*Department of Physical Sciences, Indian Institute of Science Education and Research Kolkata, Mohanpur 741246, West Bengal, India*

<sup>3</sup>*Department of Mathematical Sciences, Durham University, Durham DH1 3LE, United Kingdom*

### ABSTRACT

In what is being dubbed as the great American solar eclipse, on 21 August 2017, a total solar eclipse will sweep across the contiguous United States providing excellent opportunities for diagnostics of the Sun corona. The Sun's coronal magnetic field is notoriously difficult to observe and well-constrained theoretical computer models are therefore necessary to understand how the corona is heated to a million degrees and how coronal magnetic field structures spawn solar storms that generate severe space weather. Here we present a technique for predicting and inferring the structure of the coronal field based on a data driven solar surface flux transport model which is forward run to 21 August 2017 to predict the Sun's surface field distribution. The predicted solar surface field is subsequently utilized as input in a potential field source surface model to generate the corona. Our simulated prediction indicates the presence of two broad helmet streamers, one each in the eastern and western limb on the southern solar hemisphere and a third possible, narrow streamer on the West limb of the northern hemisphere. The (open) polar flux in the South pole appears to be stronger relative to the North, indicating an asymmetric sunspot cycle 25 with stronger activity in the southern hemisphere.

## 1. INTRODUCTION

Solar eclipses have been observed since the ancient times and have been objects of awe and wonder for human beings. While that natural reaction to a rare occurrence of nature has not changed over time, we have come to realize the immense potential for scientific investigations that eclipses provide (see e.g., [Habbal et al. \(2010\)](#)). The solar eclipse which will occur on 21 August 2017 will be the first total solar eclipse visible across the entire contiguous United States since June 8, 1918. This event, dubbed as the great American solar eclipse has generated immense interest among the general public and scientists alike. In particular, this event is expected to provide excellent opportunities for detailed observations of the Sun's coronal structure that may allow diagnostics of the underlying coronal magnetics fields.

The magnetic field configuration of the Sun's atmosphere is responsible for structuring of the million degree corona, its heating and its slow quasi-static evolution. Coronal magnetic field dynamics are also responsible for its brightness and density fluctuations. These dynamics are mediated via magnetic flux emergence and restructuring through relaxation processes and reconnection. The Sun's coronal magnetic field is also responsible for determining the heliospheric environment, specifically solar wind conditions, open magnetic flux and cosmic ray flux modulation. Eruptive events such as flares and coronal mass ejections (CMEs) associated with coronal magnetic structures generate severe space weather that may potentially impact human technologies in space and on Earth, including satellite operations, telecommunications, GPS navigational networks and electric power grids ([Schrijver et al. 2015](#)). Therefore constraining coronal magnetic field structures is of crucial importance. However, this remains an outstanding challenge even today due to the very low density and consequently low photon flux from the corona, in comparison to the solar disk. In this light, total solar eclipses – rare events wherein the Sun's bright disk is completely masked by the Moon, provide the best opportunity for ground-based coronal diagnostics.

The Sun's magnetic fields are generated in its interior through a magnetohydrodynamic (MHD) dynamo mechanism ([Parker 1955](#); [Charbonneau 2010](#)) from where they buoyantly emerge to form sunspots. In the Sun's convection zone helical turbulence twists the magnetic field lines at small-scales, and the Coriolis force tilts the axis of underlying magnetic flux tubes at large scales such that bipolar sunspots pairs or solar active regions (ARs) emerge with a tilt. Flux transport processes such as differential rotation, turbulent diffusion and meridional circulation redistribute the magnetic flux driving the surface evolution of the Sun's magnetic fields ([Wang et al. 1989b](#); [Nandy, Munoz-Jaramillo and Martens 2011](#)). Surface flux emergence, its consequent redistribution by flux transport processes drive the evolution of the Sun's coronal magnetic field – which tends to evolve and relax towards a minimum energy state in the low plasma- $\beta$  corona. The latter nonetheless hosts non-potential structures that are far from equilibrium. A variety of theoretical modelling techniques such as Potential Field Source Surface (PFSS) extrapolations, Non-linear Force-Free Field (NLFFF) extrapolations, magneto-frictional and full MHD approaches exist to model the coronal structure. A detailed description of these modeling techniques can be found in [Mackay & Yeates \(2012\)](#). In the absence of routine, quantitative coronal field observations which are rare (see e.g., [Casini, White and Judge \(2017\)](#) and references therein) these models are currently relied upon to understand the underlying magnetic field structures that drive coronal dynamics. Efforts are underway to utilize model simulations to generate synthetic polarization profiles for interpreting coronal observations in an effort to marry theory and observations ([Gibson et al. 2016](#)).

On the one hand, prediction of the coronal magnetic field structure during total eclipses utilizing theoretical models is a Rosetta stone for interpretation of the white light coronal structure visible during totality. On the other hand, the observationally inferred coronal magnetic field provides constraints on theoretical modelling efforts. A prediction of the coronal structure expected during the 21 August 2017 solar eclipse based on MHD simulations of the solar corona (utilizing photospheric magnetogram as a bottom boundary condition) has recently been made by [Predictive Science Inc.](#); see also, [Mikic et al. \(2007\)](#); [Downs et al. \(2016\)](#). These sophisticated simulations can provide details of not only the magnetic structure but also the temperature and emission profiles of the corona and are expected to render non-potential twisted structures better than other approaches. However, these simulations are numerically extremely resource heavy, rely on magnetic field maps of only the visible solar-disk (thus missing out on far-side information) and moreover, do not yet capture the impact of built in memory of the solar corona that accrues from the slow large-scale surface field evolution on timescales of years.

Here, we present an alternative modeling approach to eclipse prediction. We first utilize a data driven surface flux transport (SFT) model of the Sun with built-in memory of many years until 16 August 2017 and forward run this to 21 August 2017 (assuming no further emergence of ARs within this period). Subsequently, we use the SFT generated surface field as a bottom boundary condition in a PFSS model to extrapolate the coronal fields and thereby predict

the field structure of the 21 August 2017 solar eclipse. We describe our models and data inputs in Section 2, present our results in Section 3 and conclude with a discussion in Section 4.

## 2. DATA AND METHODS

### 2.1. Surface Flux Transport Methodology

The magnetic field evolution on the solar surface is governed by two physical processes: advection due to the large scale flows and diffusion caused by the turbulent motion of super granular convective cells. The diffusion results in the flux cancellation among the magnetic field of opposite polarities, whereas advection causes transportation of magnetic flux towards the polar regions of the Sun. This entire process is better known as Babcock-Leighton (BL) mechanism (Babcock 1961; Leighton 1969). The Surface Flux Transport (SFT) models (Wang et al. 1989b, 2000b; van Ballegooijen et al. 1998; Schrijver 2001; Mackay et al. 2002a,b; Cameron et al. 2010; Upton & Hathaway 2014a) are quite successful in capturing the physics of the BL mechanism. For constant diffusivity, the magnetic field evolution on the solar surface is governed by the magnetic induction equation,

$$\frac{\partial \mathbf{B}}{\partial t} = \nabla \times (\mathbf{v} \times \mathbf{B}) + \eta \nabla^2 \mathbf{B} \quad (1)$$

where  $\mathbf{v}$  represents the large scale velocities, i.e. meridional circulation and differential rotation present on the solar surface and the parameter  $\eta$  symbolizes the magnetic diffusivity. We have further considered that the magnetic field on the solar surface is only radial in direction. This is supported by observations that show surface magnetic fields are predominantly radial (Wang et al. 1992; Solanki 1993). We can therefore express the radial component of the induction equation in spherical polar coordinates as,

$$\frac{\partial B_r}{\partial t} = -\omega(\theta) \frac{\partial B_r}{\partial \phi} - \frac{1}{R_\odot \sin \theta} \frac{\partial}{\partial \theta} \left( v(\theta) B_r \sin \theta \right) + \frac{\eta_h}{R_\odot^2} \left[ \frac{1}{\sin \theta} \frac{\partial}{\partial \theta} \left( \sin \theta \frac{\partial B_r}{\partial \theta} \right) + \frac{1}{\sin^2 \theta} \frac{\partial^2 B_r}{\partial \phi^2} \right] + S(\theta, \phi, t) \quad (2)$$

Here  $B_r(\theta, \phi, t)$  is the radial component of magnetic field as a function of the co-latitude ( $\theta$ ) and longitude ( $\phi$ ),  $R_\odot$  is the solar radius. The axisymmetric differential rotation and meridional circulation are expressed through  $\omega(R_\odot, \theta) \approx \omega(\theta)$  and  $v(R_\odot, \theta) \approx v(\theta)$  respectively. The parameter  $\eta_h$  is the effective diffusion coefficient and  $S(\theta, \phi, t)$  is the source term describing the emergence of new sunspots. Since we are studying the evolution of  $B_r$  only on the solar surface, the code has been developed using spherical harmonics.

To represent the surface differential rotation as a function of co-latitudes we use an empirical profile (Snodgrass 1983),

$$\omega(\theta) = 13.38 - 2.30 \cos^2 \theta - 1.62 \cos^4 \theta \quad (3)$$

wherein,  $\omega(\theta)$  has units in degrees per day. This profile is validated by helioseismic observations (Schou et al. 1998). Another significant large-scale flow observed on the solar surface is the meridional circulation which carries magnetized plasma from the equatorial region towards the polar regions in both hemispheres. To replicate this flow, we have used a velocity profile prescribed by van Ballegooijen (van Ballegooijen et al. 1998) in our model.

$$v(\lambda) = \begin{cases} -v_0 \sin(\pi \lambda / \lambda_0) & \text{if } |\lambda| < \lambda_0 \\ 0 & \text{otherwise} \end{cases} \quad (4)$$

Where  $\lambda$  is the latitude in degrees ( $\lambda = \pi/2 - \theta$ ) and  $\lambda_0$  is the latitude beyond which the circulation speed becomes zero. In our model we have taken  $\lambda_0 = 75^\circ$  and  $v_0 = 15 \text{ ms}^{-1}$ . We have used a constant diffusion coefficient of  $250 \text{ km}^2 \text{s}^{-1}$  which lies within the values inferred from observations (Schrijver & Zwaan 2000).

Our newly developed SFT model utilizes the above-mentioned parameter profiles. Using this model, we have simulated the magnetic field on the solar surface from August 1913 to 21st August 2017 using observed sunspot data.

### 2.2. Sunspot Data

Modelling the emergence of sunspots requires knowledge of the following parameters: time of appearance, position on the solar surface and the area associated with the spots. The Royal Greenwich Observatory (RGO) and United

States Air Force (USAF)/National Oceanic and Atmospheric Administration (NOAA) database provides the required data on active regions from August 1913 till September 2016. Using this data, we have calibrated our SFT model by comparing model outputs with observation. The data required from 1st October 2016 to 16th August 2017 has been obtained from the Helioseismic and Magnetic Imager (HMI) aboard NASA's Solar Dynamic Observatory (SDO). The magnetogram cutouts of Spaceweather HMI Active Region Patches (SHARP) have been used in our study.

We have only considered active regions that are recognized by NOAA. We assume all sunspots appearing on the solar photosphere are Bipolar Active Regions (BMRs) of  $\beta$  type and their tilt is based on their latitudinal position (Jiang et al. 2011a). In our SFT simulation, we have used area data of ARs from both RGO-NOAA/USAF and HMI databases. We compare the maximum area reported by these two databases for all ARs that appeared during January to September 2016, and find that the area reported by HMI is higher than what RGO-NOAA/USAF has reported. Since our SFT simulation is calibrated based on 100 years (starting from 1913) of RGO-NOAA/USAF dataset, we scale down the area reported by HMI by a constant factor of 2.2 to match the RGO AR area. We determine this scaling factor by using a linear fit between the area reported by both database for the overlapping period of 9 months (January to September 2016). We note that the relative fluxes (of various BMRs and large-scale) structures is preserved in this method. The flux associated with BMRs are estimated based on an empirical relationship (Sheeley 1966; Dikpati et al. 2006):  $\Phi(A) = 7.0 \times 10^{19} A$  Maxwells, where  $A$  is the area of the whole sunspot in unit of micro-hemispheres. This flux is equally distributed among the two polarities of the BMR. The last active region that was inserted in our SFT model is AR 12671, which emerged at the surface on 16th August 2017. We then simulate the evolution of magnetic field for five more days to generate the surface magnetic field that is expected on 21st August 2017 during the eclipse.

### 2.3. PFSS Extrapolation

Due to low coronal plasma density, the photon flux is considerably lower than from the photosphere. This prevents reliable measurement of the coronal magnetic field. Therefore, to study the corona, we utilize theoretical models that simulate the magnetic field profiles in the corona using the photospheric magnetic field as a lower boundary condition.

One of the most common techniques used to simulate the corona is the Potential Field Source Surface (PFSS) extrapolation. This extrapolation assumes a current free condition in the solar corona. The magnetic field thus exists in a state of lowest energy and does not have Lorentz forces that can drive motion in the corona.

As a PFSS solution assumes a current free state, we have

$$\nabla \times \mathbf{B} = 0 \quad (5)$$

We can therefore assume  $\mathbf{B}$  to be defined based on a scalar potential ( $\Phi$ ) as

$$\mathbf{B} = \nabla \Phi \quad (6)$$

Imposing Gauss Law we obtain,

$$\nabla^2 \Phi = 0 \quad (7)$$

The PFSS solution is obtained by solving eq. 7.

Schatten, Wilcox and Ness (1969); Altschuler and Newkirk (1969) first suggested the use of the PFSS solution to study the corona. Davis (1965) further argued that magnetic fields in the plasma must become radial at the point where gas pressure starts dominating over magnetic pressure which is expected to occur at  $2.5 R_\odot$ . The magnetic fields would otherwise not be able to remain in a quasi-static state in a radially flowing plasma. Our PFSS model therefore renders the magetic field distribution between the solar surface and  $2.5 R_\odot$ . The boundary conditions to obtain the PFSS solution adopts the photospheric magnetic field as the lower boundary condition and assumes the upper boundary condition to have a radial magnetic field.

## 3. RESULTS

We use the radial magnetic field data obtained from our SFT simulation to generate the butterfly diagram (Figure 1) covering a time between the beginning of solar cycle 23 (May 1996) to 21st August 2017. We can identify the principal characteristics of the BL mechanism: cross equatorial cancelation of magnetic flux associated with the leading polarities and advection of flux from the following polarity towards the pole due to the poleward meridional circulation – which eventually results in reversal of the old cycle polar field and build-up of the new cycle field. Near the end of the simulation which corresponds to the declining phase of cycle 24, one can already see the new polarity polar field being

built up. The global, large-scale structuring of the coronal field is due to this magnetic field distribution at the solar surface, with localized perturbations imposed by the emergence of any new ARs. In our model run we have included the last observed active region on 16 August, 2017 (AR 12671) and the forward run assumed no emergence of any new ARs. The end of the simulation as depicted in Figure 1 corresponds to 21 August, 2017, the day of the solar eclipse.

The predicted surface magnetic field map of 21 August, 2017 is extracted from this simulation and is depicted in the solar disk part of the three images in Figure 2. It is seen that AR 12671 would be located just West of disk-center on the day of the eclipse and is therefore not expected to significantly affect the (projected) near-limb view of the corona (as viewed from Earth).

This surface magnetic field distribution is then utilized as an input in a PFSS model to extrapolate the coronal structure of the global Sun (Figure 2), as expected on 21 August, 2017. The inferred coronal magnetic field structure is our primary and most important prediction and is shown in Figure 2 (top). Only the open field lines reaching up to the source surface is rendered in Figure 2 (middle). A synthetic coronal white light map reconstructed using an algorithm that provides more weight (i.e., intensity) to higher density closed field lines (but without any height dependence) in depicted in Figure 2 (bottom). Based on these simulated coronal structure, we predict the existence of two helmet streamers in the mid-latitude southern solar hemisphere, one each in the East and West limb. Their locations are marked as 1 and 2 in Figure 2 (top). A third possible streamer structure (much more confined and narrow) is located in the West limb northern hemisphere (location 5). As can be seen from Figure 2 (top), these structures represent regions of closed magnetic field lines overlying the solar surface. In Figure 2 (middle) these helmet streamer structures are missing because we render only the open field lines and in Figure 2 (bottom) they appear as bright petal-like structures with pointed tips. Regions marked as 3 and 4, in the northern hemisphere West and East limb, respectively, are latitudinally extended low-lying closed magnetic field structures. These appear as somewhat flattened, large-scale diffuse bright regions in the synthetic corona rendition in Figure 2 (bottom). A comparison of the radially open magnetic field lines (which emanate from unipolar patches) from the North and South poles clearly show that the South pole has more densely packed field lines. This implies that the polar flux in the South pole is stronger relative to the North pole and is indicative that the sunspot cycle 25 will be asymmetric, with stronger sunspot activity in the southern hemisphere.

In the synthetic corona generated using our algorithm, the two helmet streamers in the South are clearly discernable. In the North, the narrow streamer-like structure on the West limb is not clearly distinguishable from the low-lying diffuse structure nearby (but may potentially be observable further out from the Sun). The coronal region overlying the northern hemisphere East limb is relatively less active compared to the others.

Figure 3 shows the global solar coronal field structure generated using the Solarsoft PFSS package. The magnetogram used for the extrapolation was acquired by HMI on 17 August, 2017 at 00:04:00 UT. The solar surface is occulted as it would appear in the eclipse. The generated coronal structure is rotated (in the direction of the Sun's rotation) by 4 days 16 hours to provide a representative structure of the corona on 21 August, 2017. While the large-scale structures are similar, a detailed comparison indicates some crucial differences. The streamers in the predicted corona from our SFT simulations are somewhat more southwards than that in Figure 3 and no difference in the density of polar field lines is apparent in Figure 3, i.e., the PFSS extrapolation employed directly on a single magnetogram.

#### 4. CONCLUDING DISCUSSION

In summary, based on a data driven solar surface flux transport simulation, forward run to 21 August, 2017, the day of the great American solar eclipse, and utilizing the predicted solar surface magnetic field map as input to a PFSS model, we have herein made a prediction of the expected coronal field structure. Our prediction is that there will be two helmet streamers (closed field structures) in the southern hemisphere, one in each limb, a third possible, narrow streamer on the northern hemisphere West limb and more diffused latitudinally extended low-lying structures in the northern hemisphere (of which, the one on the western limb is likely to be more prominent). We find a higher spatial density of open field lines in the South pole relative to the North, which is a result of stronger polar field build up in the South (leading to the minimum of the current solar cycle 24). This implies the next solar cycle 25 is likely to be asymmetric with stronger activity in the southern hemisphere.

We note that our simulated streamers in the Southern hemisphere are at higher latitudes relative to the PFSS extrapolated corona based on the single HMI magnetogram (the latter is depicted in Figure 3). We surmise that this is due to the effect of the poleward meridional circulation in our surface flux transport model and the more accurate rendering of the high latitude fields in the latter. Comparison also shows that there are distinct asymmetry in the North

and South polar coronal (open) magnetic field lines generated from the SFT simulation, which is not apparent in the PFSS extrapolation based on the magnetogram. There are some obvious qualitative agreements, as well as differences with the recent coronal structure prediction by [Predictive Science Inc.](#). The forthcoming eclipse will offer us a chance to evaluate these models and by extension our conceptual understanding of the physics driving the structuring and evolution of the solar corona.

The CESSI prediction of the coronal field expected during the 21 August, 2017 solar eclipse, accompanying images and data is available at the [CESSI prediction website](#).

This eclipse prediction campaign was conceived and led by CESSI, a multi-institutional Center of Excellence established and funded by the Ministry of Human Resource Development, Government of India. P.B. acknowledges funding by CEFIPRA/IFCPAR through grant 5004-1. S.D. acknowledges funding from the DST-INSPIRE program of the Government of India. D.N. and A.R.Y. acknowledge the NASA Heliophysics Grand Challenge Grant NNX14AO83G for facilitating their interactions. D.N. acknowledges an associateship from the Inter-University Centre for Astronomy and Astrophysics. We acknowledge utilization of data from the NASA/SDO HMI instrument maintained by the HMI team and the Royal Greenwich Observatory/USAF-NOAA active region database compiled by David H. Hathaway.

## REFERENCES

Altschuler, M. D. and Newkirk, G. , 1969, Solar Physics, 9, 131

Babcock, H. W., 1961, ApJ, 133, 572

Cameron, R. H., Jiang, J., Schmitt, D. & Schüssler, M., 2010, ApJ, 719, 264

Casini, R., White, S.M. and Judge, P.G., 2017, Space Science Review.

Charbonneau, P., 2010, Living Reviews in Solar Physics, 7, 3.

Davis, L., 1965, Stellar and Solar Magnetic Fields, North Holland Publishing Co.

Dikpati, M., de Toma, G., & Gilman, P. A. 2006, GeoRL, 33, 5102

Gibson, S., Kucera, T., White, S., Dove, J., Fan, Y., Forland, B., Rachmeler, L., Downs, C., Reeves, K., 2016, FORWARD: A toolset for multiwavelength coronal magnetometry, 3.

Downs, C., Lionello, R., Miki, Z., Linker, J. A. and Velli, M., 2016, ApJ, 832, 180.

Habbal, S.R., Druckmller, M., Morgan, H., Scholl, I., Ruin, V., Daw, A., Johnson, J. and Arndt, M., 2010, ApJ, 719, 1362

Hathaway, D. H. & Rightmire, L., 2011, ApJ, 729, 80

Jiang, J., Cameron, R. H., Schmitt, D., & Schüssler, M. 2011, A&A, 528, A82

Leighton, R. B. 1969, ApJ, 156, 1

Mackay, D. H., Priest, E. R. and Lockwood, M., 2002a, SoPh, 207, 291

Mackay, D. H., Priest, E. R. and Lockwood, M., 2002a, SoPh, 209, 287

Mackay, D., & Yeates, A. 2012, LRSP, 9, 6

Mikic, Z., Linker, J. A., Lionello, R., Riley, P. and Titov, V., 2016, ASP Conference Series, 370, 299.

Nandy, D., Munoz-Jaramillo, A. and Martens, P.C.H., 2011, Nature, 471, 8082

Parker, E.N., 1955, ApJ, 122, 293.

Schatten, K. H., Wilcox, J. M. and Ness, N. F., 1969, Solar Physics, 6, 442

Schou, J., Antia, H. M., Basu, S., Bogart, R. S., Bush, R. I., Chitre, S. M., Christensen-Dalsgaard, J., Di Mauro, M. P., Dziembowski, W. A., Eff-Darwich, A., Gough, D. O., Haber, D. A., Hoeksema, J. T., Howe, R., Korzennik, S. G., Kosovichev, A. G., Larsen, R. M., Pijpers, F. P., Scherrer, P. H., Sekii, T., Tarbell, T. D., Title, A. M., Thompson, M. J. & Toomre, J., 1998, /apj, 505, 390

Schrijver, C.J., 2001, ApJ, 547, 475

Schrijver, C.J., DeRosa, M.L. and Title, A.M., 2002, ApJ, 577, 1006

Schrijver, C.J. & Zwaan, C., 2000, Solar and Stellar Magnetic Activity, vol. 34 of Cambridge Astrophysics Series, Cambridge University Press

Schrijver, C. J., Kauristie, K., Aylward, A. D., Denardini, C. M., Gibson, S. E., Glover, A., and Jakowski, N., 2015, Advances in Space Research, 55(12), 2745-2807.

Sheeley, N.R., Jr., 1966, ApJ, 144, 723

Snodgrass, H.B., 1983, ApJ, 270, 288

Solanki, S. K., 1993, Space Sci. Rev., 63, 1

Upton, L. & Hathaway, D. H., 2014a, ApJ, 780, 5

van Ballegooijen, A.A., Cartledge, N.P. & Priest, E.R., 1998, ApJ, 501, 866

Wang, Y.-M., Nash, A.G. & Sheeley Jr, N.R., 1989b, Science, 245, 712

Wang, Y.-M., Sheeley Jr., N. R. & Lean, J., 2000b,  
Geophys. Res. Lett., 27, 621  
Wang, Y.-M. & Sheeley Jr., N. R. 1992, ApJ, 392, 310

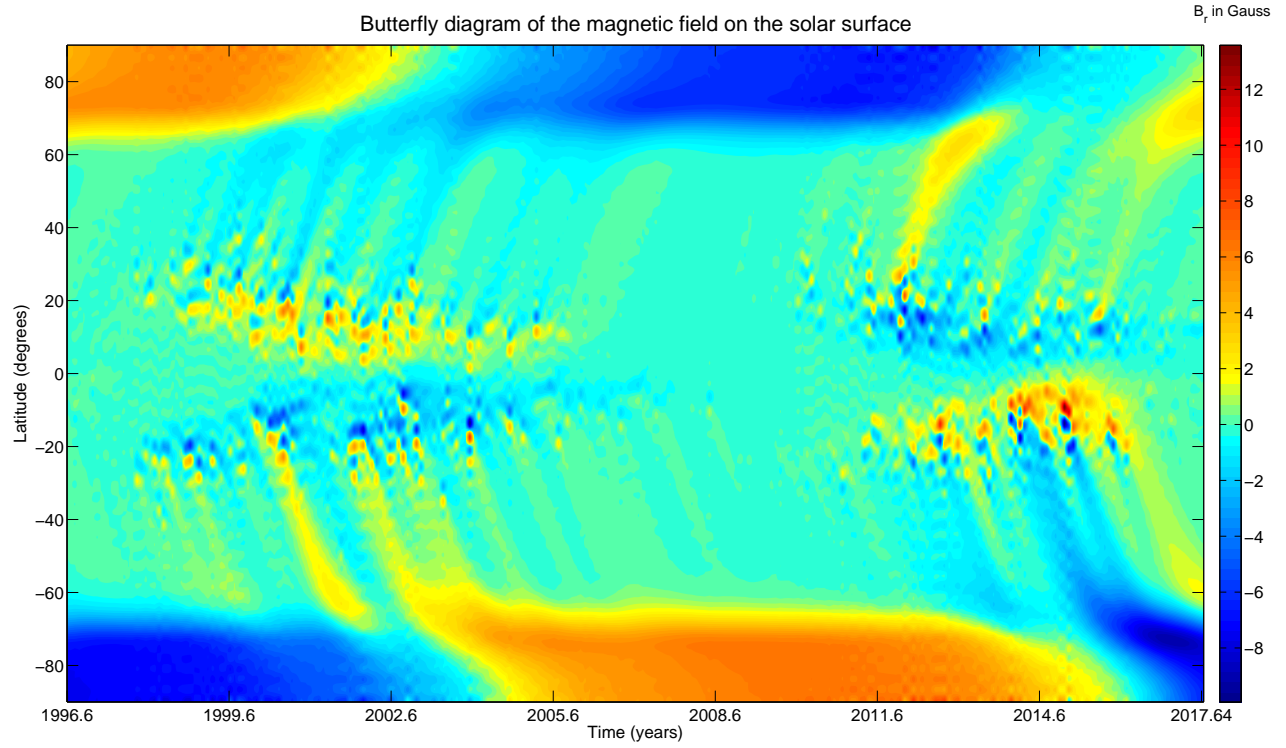


**Figure 1.** The above figure depicts the evolution of surface magnetic field during the last decade generated from our SFT simulation. The radial component of longitudinally averaged magnetic field ( $B_r$ ) is plotted as a function of time and latitude. The color bar represents the strength of the magnetic field in Gauss.

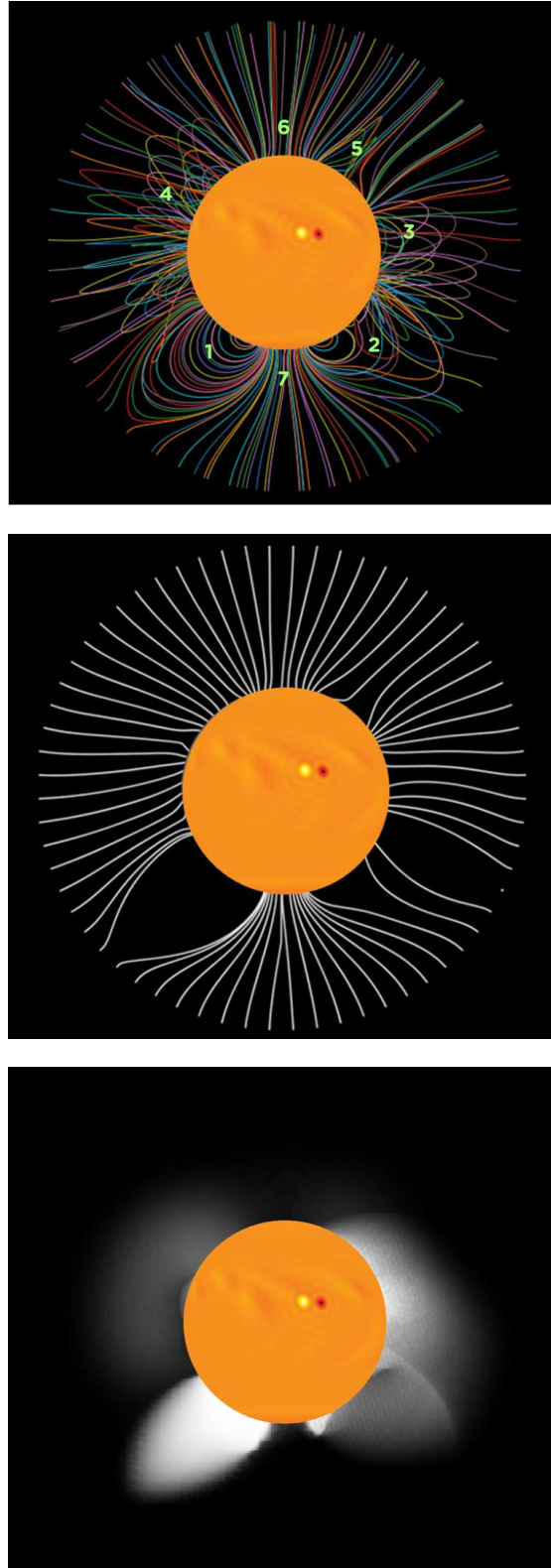


**Figure 2.** Top panel: This image depicts a rendering of the open and closed solar coronal magnetic field lines generated using a PFSS model which utilized the predicted surface magnetic field map from a SFT model forward run to 21 August, 2017, i.e., the day of the eclipse. Middle panel: Only the open magnetic field lines reaching up to the source surface at  $2.5 R_{\odot}$  are depicted in this image. Bottom panel: Shows a synthetic map of the white light corona expected during the eclipse, in which the intensity of the image is dependent on the density of closed field lines; open field lines are assigned zero intensity and there is no height dependence incorporated. Thus, this should be interpreted only as a guide-to-the-eye for the latitudinal location of the brightest large-scale coronal structures. In all images, solar North is up.

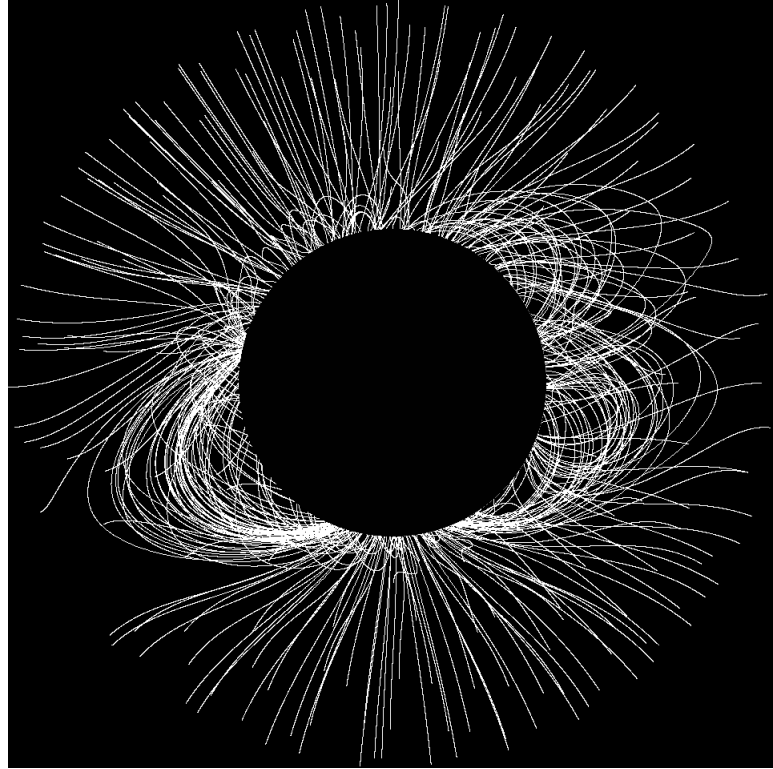


**Figure 3.** This image shows the Potential Field Source Surface (PFSS) extrapolation model output on the HMI magnetogram of 17 August 2017 acquired at 00:04:00 UT, after rotation of the coronal fields by 4 days 16 hours. This rotation is implemented to approximately capture the coronal structure expected on the day of the eclipse, i.e., 21 August, 2017. The field lines extend till  $2.5 R_{\odot}$ . The surface of the sun is occulted for better visualization of the global coronal structure. This coronal field extrapolation is rendered by the PFSS package available in the Solarsoft Library.